B cell-derived IL-10 suppresses inflammatory disease in Lyn-deficient mice

Patrizia Scapini[a,b,1], Chrystelle Lamagna[a], Yongmei Hu[a], Karim Lee[c], Qizhi Tang[c], Anthony L. DeFranco[d], and Clifford A. Lowell[a,1]

Departments of [a]Laboratory Medicine and [d]Microbiology/Immunology, University of California, San Francisco, CA 94143; [b]Department of Pathology and Diagnostics, Division of General Pathology, University of Verona, 37134 Verona, Italy; and [c]Diabetes Center and Departments of Medicine and Surgery, University of California, San Francisco, CA 94143

Lyn kinase deficient mice represent a well established genetic model of autoimmune/autoinflammatory disease that resembles systemic lupus erythematosus. We report that IL-10 plays a crucial immunosuppressive role in this model, modulating the inflammatory component of the disease caused by myeloid and T-cell activation. Double-mutant $lyn^{-/-}IL-10^{-/-}$ mice manifested severe splenomegaly and lymphadenopathy, dramatically increased proinflammatory cytokine production, and severe tissue inflammation. Single-mutant $lyn^{-/-}$ mice showed expansion of IL-10–producing B cells. Interestingly, WT B cells adoptively transferred into $lyn^{-/-}$ mice showed increased differentiation into IL-10–producing B cells that assumed a similar phenotype to endogenous $lyn^{-/-}$ IL-10–producing B cells, suggesting that the inflammatory environment present in $lyn^{-/-}$ mice induces IL-10–producing B-cell differentiation. B cells, but not T or myeloid cells, were the critical source of IL-10 able to reduce inflammation and autoimmunity in double mutant $lyn^{-/-}IL-10^{-/-}$ mice. IL-10 secretion by B cells was also crucial to sustain transcription factor Forkhead Box P3 (Foxp3) expression in regulatory T cells during disease development. These data reveal a dominant immunosuppressive function of B-cell–derived IL-10 in the Lyn-deficient model of autoimmunity, extending our current understanding of the role of IL-10 and IL-10–producing B cells in systemic lupus erythematosus.

signal transduction | tyrosine kinase | B regulatory cells

Systemic lupus erythematosus (SLE) is a complex autoimmune disorder that involves many facets of the immune system and is thought to result from the interaction between genetic and environmental factors (1). Conventional models consider SLE to be primarily caused by B-cell hyperactivity, production of autoantibodies, and immune complex deposition (2). However, mounting evidence has indicated an important pathological role of T cells (3) and, more recently, myeloid cells (4, 5) in this disease. Impaired cytokine production and deregulated inflammation, including altered responses to Toll-like receptor ligand stimulation, have also been shown to be major contributors to tissue injury and end-organ damage in this disease (6–8).

Several murine models of human SLE have been developed (9). The Lyn-deficient model of SLE-like disease is a single gene defect model that results in hyperactive intracellular signaling responses (10, 11). Mutations in the *LYN* gene have been associated with SLE in humans (12). Lyn kinase is expressed mainly in B and myeloid cells, and its deficiency in mice leads to progressive autoimmunity characterized by autoantibody production, lymphocyte activation, immune complex deposition, and nephritis (10). $Lyn^{-/-}$ B cells are hyperactive to antigen receptor stimulation, which leads to abnormal B-cell selection and/or tolerance, resulting in the production of self-reactive antibodies (10, 13). $Lyn^{-/-}$ myeloid cells are also hyperresponsive to various stimuli, and recent evidence suggests that these cells are major contributors to disease development (11, 14, 15). In particular, overproduction of B-cell–activating factor of the TNF family (BAFF) by $lyn^{-/-}$ myeloid cells is fundamental in this model to sustain not

only B-cell, but also T-cell activation. It is clear that the SLE-like disease in this model is characterized not only by autoantibody production and hyperactivated B cells, but also by pathogenic interactions between myeloid cells and T cells that sustain inflammation, disease progression, and nephritis development (14).

IL-10 is an antiinflammatory cytokine with a crucial role in controlling inflammatory responses that cause tissue damage. IL-10 exerts its suppressive role primarily by limiting innate effector functions of macrophages and dendritic cells (DCs; including proinflammatory cytokine production by the latter cells in response to Toll-like receptor ligands) and their subsequent activation of T cells. The potent role of IL-10 as immunosuppressive/antiinflammatory cytokine has been proven by the fact that IL-10 deficiency strongly exacerbates certain types of autoimmune diseases, such as inflammatory bowel disease and multiple sclerosis (which are typically considered as T-cell–mediated autoimmune diseases) (16–18). On the contrary, besides its immunosuppressive functions, IL-10 is also known to boost B-cell proliferation and Ig class switching, resulting in enhanced antibody secretion. As a consequence, the contribution of IL-10 to SLE pathogenesis is less clear (16, 19, 20). An important role of IL-10 in T-cell–mediated immune regulation has been linked to CD4^{+} CD25^{+} Forkhead Box P 3 (Foxp3)[+] regulatory T cells (Tregs) (21). The importance of IL-10 production by Tregs as a mechanism for their suppressive functions is controversial and dependent on the experimental system (21, 22). However, IL-10 has recently been found to play a crucial role in maintaining Treg-suppressive function under inflammatory conditions by preventing the down-regulation of Foxp3 expression (23). A reduction in Foxp3 levels is associated with loss of Treg-suppressive function, generation of pathogenic Tregs that may express IL-17 and/or IFN-γ, and increased susceptibility to autoimmunity (24–26). A protective role of CD4^{+} CD25^{+}Foxp3^{+} Tregs in murine models of SLE has also been reported (27, 28).

Recently, B cells with regulatory suppressive activity, also known as regulatory B cells (Bregs), have been discovered in several mouse models of inflammation and autoimmunity, such as contact hypersensitivity, inflammatory bowel disease, experimental autoimmune encephalomyelitis, collagen-induced arthritis, and type I diabetes (29–31). This conclusion was derived from the paradoxical observation that depletion of B cells leads to exacerbation of disease processes in some of these models.

Accumulating evidence suggests that B cells exert their regulatory role mainly through the production of IL-10. Various subsets of B cells have been found to produce IL-10, and the number of these cells is increased in the aforementioned models, but generally they represent less than 10% of the total B-cell population (29–31). B-cell–derived IL-10 has also been implicated in balancing immune responses to pathogens (32). Recently, immunosuppressive subsets of B cells have been implicated in modulation of SLE-like disease in mice; however, it is unclear if this is a result of IL-10 production (33–35). Clearly, the concept that B cells have important regulatory functions in immune responses, beyond just antibody production, is an emerging theme.

In the present study, we used the Lyn-deficient model of autoimmunity to further elucidate the role of IL-10, and IL-10–producing cell subsets, in the modulation of SLE. We found that IL-10 plays a crucial role in modulating the inflammatory component of the disease caused by myeloid and T-cell activation in this model. Surprisingly, despite the well characterized pathological role of B cells in Lyn-deficient autoimmunity, we identified the latter cells as the critical IL-10–producing cell type

capable of restraining inflammation and disease progression in $lyn^{-/-}IL10^{-/-}$ mice.

Results

IL-10 Deficiency Dramatically Increases Splenomegaly and Lymphadenopathy in $lyn^{-/-}$ Mice. With age, $lyn^{-/-}$ mice develop an inflammatory and autoimmune disease that is characterized by increased production of proinflammatory cytokines such as BAFF, IFN-γ, and IL-6 (14, 36). Serum levels of the anti-inflammatory cytokine IL-10 were also elevated in $lyn^{-/-}$ mice at 2 mo of age and progressively increased, reaching a plateau at approximately 4–6 mo of age (Fig. 1A). We therefore decided to investigate the effect of IL-10 deficiency on the inflammatory/autoimmune disorder developed by $lyn^{-/-}$ mice by generating animals deficient for both Lyn and IL-10 ($lyn^{-/-}IL-10^{-/-}$ mice). Whereas $lyn^{-/-}$ mice are long-lived, $lyn^{-/-}IL-10^{-/-}$ double-mutant mice showed a striking increase in mortality compared with control animals; the survival rate at 6 mo was only 25% for $lyn^{-/-}IL-10^{-/-}$ mice, compared with 75% for $IL-10^{-/-}$ mice and 100% for WT and $lyn^{-/-}$ mice. Furthermore, the birth rate of the double-mutant mice was much
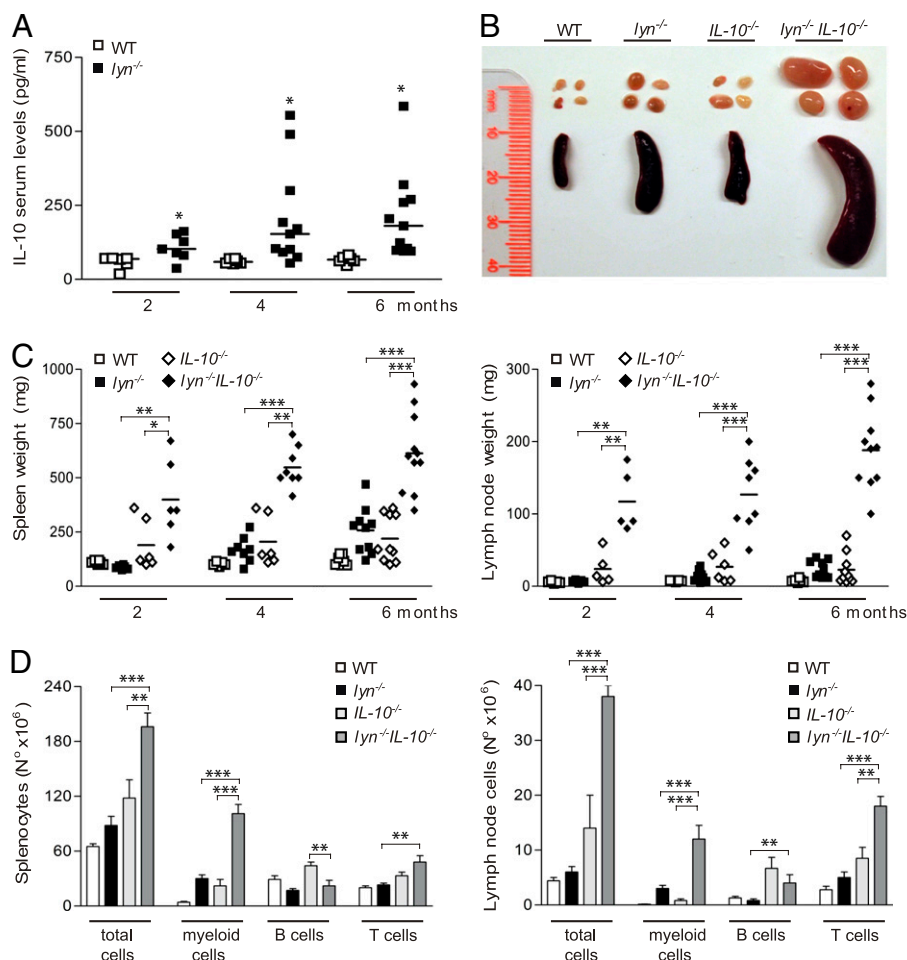

Fig. 1. $Lyn^{-/-}$ mice have increased IL-10 serum levels and manifest dramatic splenomegaly and lymphadenopathy as a consequence of IL-10 deficiency. (A) ELISA of IL-10 serum levels in 2-, 4-, and 6-month-old WT or $lyn^{-/-}$ mice. Each symbol represents the IL-10 serum level of an individual mouse. Data are pooled from two independent time-course experiments. (B) Representative images of spleen and lymph nodes from 5- to 6-mo-old WT, $lyn^{-/-}$, $IL-10^{-/-}$, or $lyn^{-/-}IL-10^{-/-}$ animals. Data are representative of 10 to 12 mice for each genotype analyzed at end-point experiments. (C) Each symbol represents the weight of an individual spleen (*Left*) or lymph node (*Right*) from 2-, 4-, and 6- month old WT, $lyn^{-/-}$, $IL-10^{-/-}$, or $lyn^{-/-}IL-10^{-/-}$ mice. Data are pooled from two independent time-course experiments. (D) Single-cell suspensions of spleens (*Left*) and lymph nodes (*Right*) from 6-mo-old WT, $lyn^{-/-}$, $IL-10^{-/-}$, and $lyn^{-/-}IL-10^{-/-}$ mice were prepared, counted, and stained for flow cytometric analysis. The absolute number of total, myeloid (CD11b$^+$), total B (CD19$^+$ *plus* CD19/B220$^{low/-}$CD138$^+$ cells), and T (TCRβ^+) cells is reported. Data are pooled from two separate time-course experiments and are expressed as mean $\pm$ SEM (n = 8–12 mice per time point). Statistical differences of $lyn^{-/-}IL-10^{-/-}$ double-mutant *versus* $lyn^{-/-}$ or $IL-10^{-/-}$ single-mutant mice are reported (*P < 0.05; **P < 0.01; ***P < 0.001).

lower, and the animals had to be bred by using IL-10 heterozygous parents. $Lyn^{-/-}IL\text{-}10^{-/-}$ mice manifested dramatic splenomegaly and lymphadenopathy starting at a young age, which were markedly more severe than in WT, $lyn^{-/-}$, or $IL\text{-}10^{-/-}$ control animals (Fig. 1 B and C). The splenomegaly and lymphadenopathy were primarily caused by a large expansion in the numbers of myeloid (CD11b$^+$) and T (TCRβ$^+$) cells (Fig. 1D). The B-cell lymphopenia normally observed in $lyn^{-/-}$ mice was not significantly altered in the spleen by IL-10 deficiency, whereas the total number of B cells was significantly increased in the lymph nodes of the double-mutant mice compared with the $lyn^{-/-}$single-mutant mice (Fig. 1D). Overall, these data suggest that IL-10 is an important negative regulator of myeloid and T-cell proliferation in $lyn^{-/-}$ mice, and lack of this cytokine severely exacerbates the development of splenomegaly and lymphadenopathy in these animals.

Finally, histological analysis of several tissues revealed a dramatic increase in inflammatory leukocyte infiltration in the kidneys, the liver, and the lungs of $Lyn^{-/-}IL\text{-}10^{-/-}$ animals compared with WT, $lyn^{-/-}$, or $IL\text{-}10^{-/-}$ control animals (Fig. S1A). These data suggest that the increased mortality observed in $lyn^{-/-}IL\text{-}10^{-/-}$ mice, compared with $lyn^{-/-}$ or $IL\text{-}10^{-/-}$ single-mutant mice, is likely caused by an increased systemic inflammatory response that affects multiple organs and tissues. However, the development of spontaneous colitis, typically caused by IL-10 deficiency, was not significantly increased in $lyn^{-/-}IL\text{-}10^{-/-}$ compared with $IL\text{-}10^{-/-}$ mice (Fig. S1A, $Bottom$, and Fig. S1 B and C).

IL-10 Deficiency Increases T-Cell, but Not B-Cell, Activation in $lyn^{-/-}$ Mice.

The hyperactivated phenotype of $lyn^{-/-}$ B cells and the contribution of these cells to autoimmunity in $lyn^{-/-}$ mice have been well described (10). Even though T cells do not express Lyn, $lyn^{-/-}$ mice have increased numbers of activated effector T cells expressing pathogenic cytokines, such as IFN-γ, and an expansion of Tregs (14, 37). Despite the positive role of IL-10 in supporting B-cell activation and antibody production (17, 18, 20), we found that the phenotype of $lyn^{-/-}$ B cells was only minimally affected by IL-10 deficiency in terms of B-cell phenotype, activation, and serum levels of autoreactive and total antibodies (Fig. S2 A–D). Furthermore, although IgG levels were increased, IL-10 deficiency did not significantly affect glomerular IgG immune complex and complement factor 3 (C3) deposits in the kidneys (Fig. S2E). However, the number of activated (CD69$^+$) and effector (CD44^{high}CD62L$^-$) T cells (both CD4$^+$ and CD8$^+$) was strongly increased in the spleens of $lyn^{-/-}IL\text{-}10^{-/-}$ compared with $lyn^{-/-}$ mice (Fig. 2A). The double-mutant animals also had a significantly increased number of IFN-γ$^+$ T cells, as well as IL-17$^+$ T cells, compared with single-mutant or WT mice (Fig. 2A). Importantly, although the frequency and total number of Tregs was increased in the spleens of $lyn^{-/-}IL\text{-}10^{-/-}$ compared with $lyn^{-/-}$ mice, the expression level of Foxp3 in these cells was significantly reduced compared with single-mutant $lyn^{-/-}$ or $IL\text{-}10^{-/-}$ mice (Fig. 2 B–D). Taken together, these data demonstrate that IL-10 plays a fundamental role in restraining T-cell activation and maintaining Foxp3 expression levels in CD4$^+$ CD25$^+$Foxp3$^+$ Tregs in $lyn^{-/-}$ mice. In contrast, IL-10 deficiency did not significantly affect B-cell activation in the Lyn-deficient model of autoimmunity.

Production of Proinflammatory Cytokines Is Increased in $lyn^{-/-}IL\text{-}10^{-/-}$ Mice.

IL-10 is a well known suppressor of proinflammatory cytokine production by several cell types, including myeloid cells (17, 18). Deregulation of cytokine production plays an important role in the inflammatory/autoimmune disease developed by $lyn^{-/-}$ mice (14, 36). We therefore investigated whether IL-10 deficiency caused increased proinflammatory cytokine production in $lyn^{-/-}$ mice by affecting, in particular, the hyperactivated $lyn^{-/-}$ myeloid
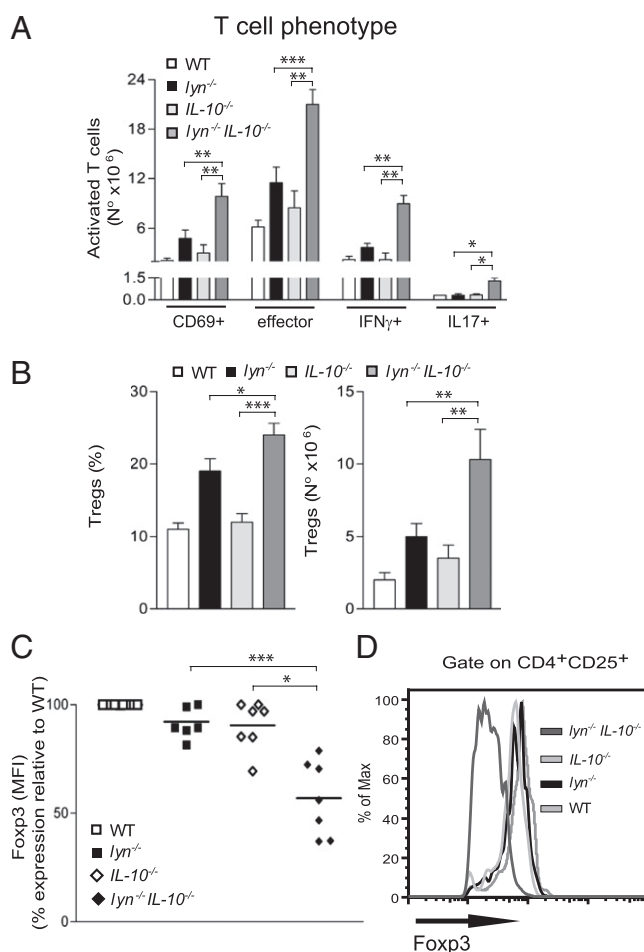

Fig. 2. IL-10 deficiency increases T-cell activation in $lyn^{-/-}$ mice. (*A*–*C*) Single-cell suspensions of spleens from 5- to 6-mo-old WT, $lyn^{-/-}$, $IL\text{-}10^{-/-}$, and $lyn^{-/-}IL\text{-}10^{-/-}$ mice were counted and stained for flow cytometric analysis. (*A*) The absolute number of TCRβ$^+$CD69$^+$, TCRβ$^+$CD44^{high}CD62L$^-$ (effector cells), TCRβ$^+$IFNγ$^+$, and TCRβ$^+$IL-17$^+$ cells is reported as evidence of T-cell activation. (*B*) The frequency (*Left*) and absolute number (*Right*) of splenic CD4$^+$CD25$^+$Foxp3$^+$ Tregs are reported. Data are pooled from three independent end-point experiments and are expressed as mean ± SEM (*n* = 8– 12 mice per group). (*C*) Each symbol represents the mean fluorescence intensity (MFI) of Foxp3 expression in splenic CD4$^+$CD25$^+$Foxp3$^+$ Tregs (calculated as percentage of MFI expression relative to WT levels for each experiment) from individual $lyn^{-/-}$, $IL\text{-}10^{-/-}$, or $lyn^{-/-}IL\text{-}10^{-/-}$ animals. Data are pooled from two independent end-point experiments. (*D*) Representative FACS histograms showing the MFI expression of Foxp3 in splenic CD4$^+$CD25$^+$Foxp3$^+$ Tregs from mice of the indicated genotype. Data are representative of five to 10 mice for each genotype. Statistical differences of $lyn^{-/-}IL\text{-}10^{-/-}$ double-mutant *versus* $lyn^{-/-}$ or $IL\text{-}10^{-/-}$ single mutant mice are reported (*P < 0.05; **P < 0.01; ***P < 0.001).

cells. Serum levels of all of the proinflammatory cytokines tested (e.g., TNF-α, IL-6, IL-12, IFN-γ, IL-1α/β, BAFF) were strongly elevated in the serum of $lyn^{-/-}IL\text{-}10^{-/-}$ compared with $lyn^{-/-}$ mice (Fig. 3 A and B). Although T cells were the likely source of the increased IFN-γ and IL-17 in the $lyn^{-/-}IL\text{-}10^{-/-}$ mice (Fig. 2A), the dramatic expansion of the hyperactivated $lyn^{-/-}$ CD11b$^+$ myeloid cell subtypes (including granulocytes, monocytes, DCs, and macrophages; Fig. 3C) could account for the overproduction of other cytokines. In line with this hypothesis, the mRNA expression levels of cytokines such as BAFF and IL-6 were increased in macrophages and DCs purified from the spleens of $lyn^{-/-}IL\text{-}10^{-/-}$ mice compared with $lyn^{-/-}$ or $IL\text{-}10^{-/-}$ animals (Fig. 3D). Similarly, myeloid cells from $lyn^{-/-}IL\text{-}10^{-/-}$ mice produced in-
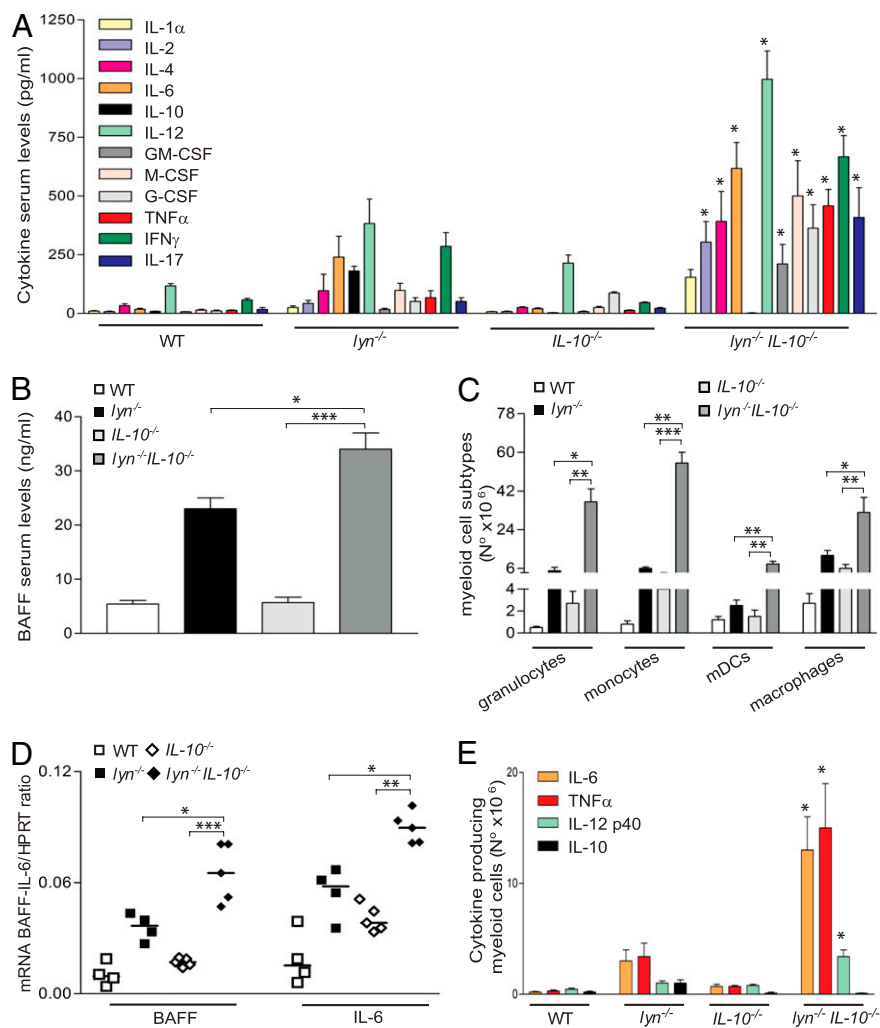
Fig. 3. IL-10 deficiency exacerbates the production of proinflammatory cytokines in $lyn^{-/-}$ mice. Serum levels of the indicated cytokines (A) and BAFF (B) in 5- to 6-mo-old WT, $lyn^{-/-}$, $IL-10^{-/-}$, or $lyn^{-/-}IL-10^{-/-}$ mice, assessed by fluorescent bead-based Luminex assays or ELISA, respectively. Data are pooled from three independent end-point experiments and are expressed as mean ± SEM (n = 8–12 mice per group). (C) Single-cell suspensions of spleens from 5- to 6-mo-old WT, $lyn^{-/-}$, $IL-10^{-/-}$, and $lyn^{-/-}IL-10^{-/-}$ mice were counted and stained for flow cytometric analysis. The absolute number of the different subsets of CD11b$^+$ myeloid cells was obtained by analyzing the expression of the following markers: CD11b^{high}7/4^{int}GR-1^{high} (granulocytes), CD11b^{high}7/4^{high}GR-1^{low} (monocytes), CD11b$^+$F4/80$^+$ (macrophages), and CD11b$^+$CD11c^{high} (myeloid DCs; mDCs). Data are from one end-point experiment and are expressed as mean ± SEM (n = 4–5 mice per group). (D) Each symbol represents BAFF or IL-6 mRNA expression in splenic macrophages and DCs purified from the spleens of individual 5- to 6-mo-old WT, $lyn^{-/-}$, $IL-10^{-/-}$, and $lyn^{-/-}IL-10^{-/-}$ mice as described in Methods. Data are pooled from two end-point experiments. (E) The absolute number of IL-6$^+$, TNF-α$^+$, IL-12 p40$^+$, and IL-10$^+$ CD11b$^+$ myeloid cells in the spleen of 5- to 6-mo-old WT, $lyn^{-/-}$, $IL-10^{-/-}$, or $lyn^{-/-}IL-10^{-/-}$ mice was determined by FACS analysis as described in Methods. Data are pooled from two end-point experiments and are expressed as mean ± SEM (n = 4–5 mice per group). Statistical differences of $lyn^{-/-}IL-10^{-/-}$ double-mutant vs. $lyn^{-/-}$ or $IL-10^{-/-}$ single mutant mice are reported (*P < 0.05; **P < 0.01; ***P < 0.001).

creased amounts of proinflammatory cytokines after LPS stimulation, as revealed by intracellular staining (Fig. 3E). These data suggest that IL-10 deficiency causes an increase in the production of proinflammatory cytokines and that $lyn^{-/-}$ myeloid cells are important contributors to the inflammatory phenotype in $lyn^{-/-}IL-10^{-/-}$ animals.

IL-10–Producing B Cells Are Increased in Spleen of $lyn^{-/-}$ Mice. Several cellular sources of IL-10, including B cells, T cells, and myeloid cells, have been identified in mouse models of inflammatory and autoimmune disease (17, 18). To detect IL-10 production in vivo, we crossed $lyn^{-/-}$ animals with the IL-10 reporter GFP knock-in "tiger" mice, which, as previously shown by Kamanaka et al., are a valuable tool for following IL-10 production as GFP expression fairly reports the IL-10 expression, but with much higher sensitivity than intracellular staining and without the necessity of performing ex vivo restimulation of

the cells (38). Consistent with the increased IL-10 serum levels observed in $lyn^{-/-}$ mice, we found that the frequency of IL-10–GFP$^+$ splenic leukocytes was significantly higher in 2-mo-old $lyn^{-/-}$tiger mice than in control tiger mice and further increased over time, reaching a plateau at approximately 4 to 6 mo of age (Fig. 4A). We also found an increased frequency of IL-10–GFP$^+$ cells in the peripheral blood, lymph nodes, bone marrow, and peritoneal cavity of $lyn^{-/-}$tiger mice compared with control tiger animals, but the overall frequency of IL-10–GFP$^+$ cells in these tissues was less than 2%. We therefore decided to focus our attention on the characterization of splenic IL-10–GFP$^+$ cells, as the spleen is the earliest tissue affected by the inflammatory/autoimmune process in this model. B cells were the main cell type expressing IL-10–GFP$^+$ (both as frequency and absolute number) in the spleens of 2-mo-old control tiger as well as $lyn^{-/-}$tiger mice (Fig. S3 A and B), consistent with previous observations made in a different IL-10 reporter mouse (39). The remaining
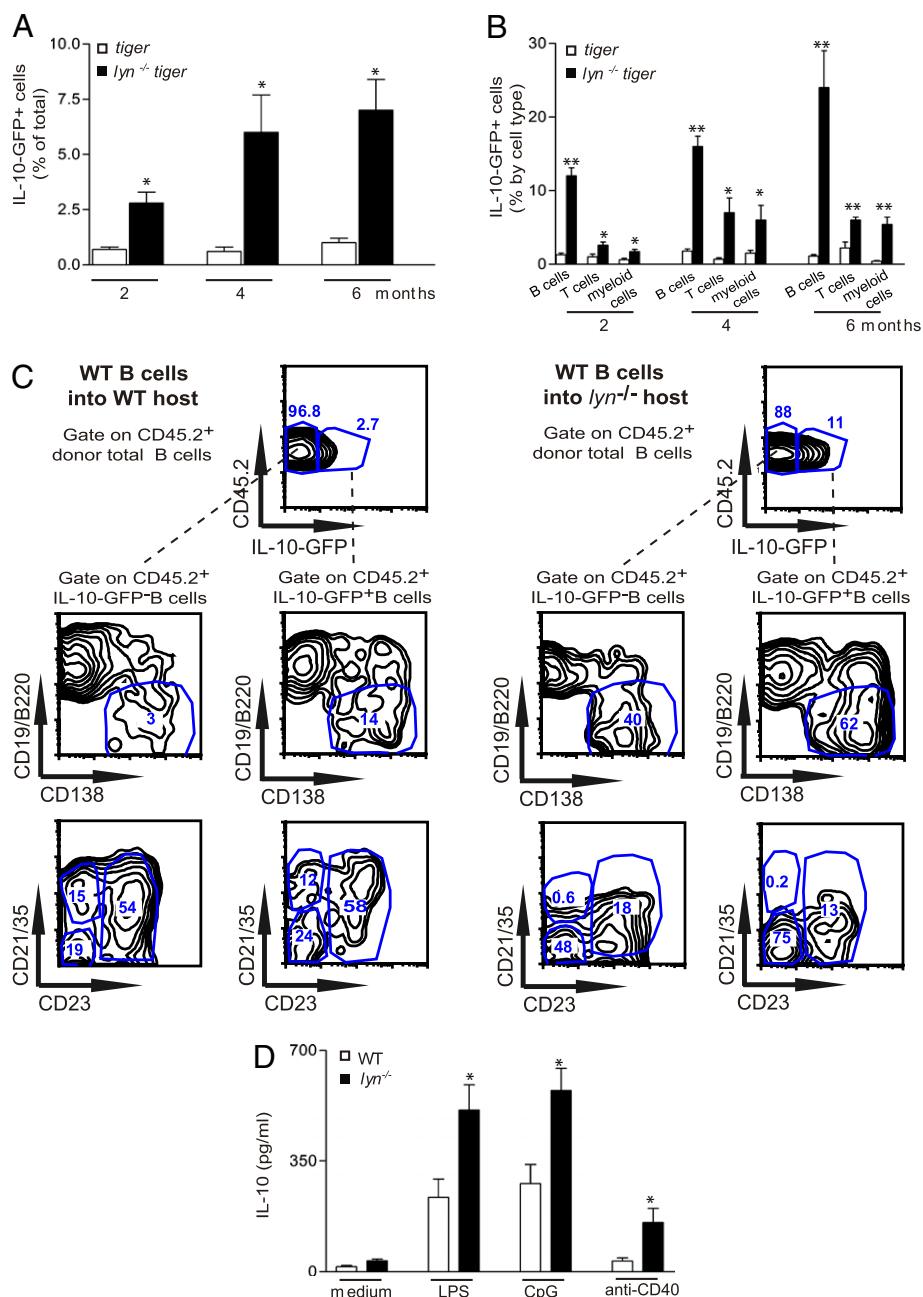
Fig. 4. The frequency of IL-10–producing B cells is increased in $lyn^{-/-}$ mice. (*A*–*C*) Single-cell suspensions of spleens from 2-, 4-, and 6-mo-old control *tiger* or $lyn^{-/-}$*tiger* mice were stained for flow cytometric analysis. The gates designed to analyze GFP expression were set by using regular WT or $lyn^{-/-}$ mice as GFP⁻ controls. (*A*) The frequency of total IL-10–GFP⁺ cells (among total splenocytes). (*B*) The frequency of IL-10–GFP⁺ B cells (among total CD19⁺ *plus* CD19/B220$^{low/-}$ CD138⁺ cells), IL-10–GFP⁺ T cells (among total TCRβ⁺ cells), and IL-10–GFP⁺ myeloid cells (among total CD11b⁺ cells). Data are pooled from two separate time course experiments and are expressed as mean ± SEM (*n* = 6–8 mice per group). Statistical differences of $lyn^{-/-}$*tiger* vs. control *tiger* mice are reported (*$P <$ 0.05; **$P <$ 0.01). (*C*) Resting CD19⁺ B cells were sorted from single-cell suspensions of spleens and lymph nodes from control *tiger* (CD45.2⁺) mice, and 10 × 10⁶ were injected i.v. into 6-mo-old congenic CD45.1⁺ WT or $lyn^{-/-}$ mice. Representative flow plots of the frequency (of total CD45.2⁺ CD19⁺ *plus* CD19/B220$^{low/-}$ CD138⁺ donor B cells) and the phenotype (expression of CD138, CD21, and CD23) of the donor CD45.2⁺IL-10–GFP⁻ B cells or CD45.2⁺IL-10–GFP⁺ B cells detected in the spleen of host CD45.1⁺ WT (*Left*) or $lyn^{-/-}$mice (*Right*) 1 mo after the adoptive transfers. Data are representative of four mice for each condition. (*D*) IL-10 protein release, assessed by ELISA, by CD19⁺ B cells isolated from spleen and lymph nodes of 2-mo-old WT or $lyn^{-/-}$ mice and stimulated for 72 h in the presence or absence of 5 μg/mL LPS, CpG oligonucleotide, or anti-CD40 Abs.

splenic IL-10–GFP⁺ cells were mainly T cells in control *tiger* mice, whereas they were both T cells and myeloid cells in $lyn^{-/-}$*tiger* mice. However, whereas, in *tiger* mice, the distribution of IL-10–GFP⁺ cells remained unchanged over time, as $lyn^{-/-}$*tiger* mice aged, the absolute number of splenic IL-10–GFP⁺ B, T, and myeloid cells increased, correlating with the overall expansion of the T and

myeloid cell compartments (Fig. S3*B*). We then analyzed the percentage of IL-10–GFP⁺ cells in a given splenic cell population and found that the frequency of IL-10–GFP⁺ B cells present in $lyn^{-/-}$*tiger* mice was much higher than in control *tiger* mice: greater than 10% of B cells were IL-10–GFP⁺, and this increased to more than 20% by 6 mo of age (Fig. 4*B*). The absolute number of IL-10–

GFP$^+$ B cells was also significantly increased in $lyn^{-/-}tiger$ mice compared with control $tiger$ mice, even though, similar to regular $lyn^{-/-}$ mice, $lyn^{-/-}tiger$ mice have a lower B-cell frequency (Fig. S3B). Among the total splenic B-cell population (gated on CD19$^+$ plus CD19/B220$^{low/-}$CD138$^+$ cells; Fig. S3C), the majority of IL-10–GFP$^+$ B cells in control $tiger$ mice were follicular (Fo) B cells and plasma cells/plasmablasts (Table 1 and Fig. S3C, Left). In contrast, in $lyn^{-/-}tiger$ mice, the majority of the IL-10–GFP$^+$ B cells were plasma cells/plasmablasts, transitional type 1 and 2 (T1,2) B cells, and B1a/b B cells (Table 1 and Fig. S3C, Right). Within the IL-10–GFP$^+$ B1 cell subsets, there was a significant reduction of CD5$^+$ IL-10–GFP$^+$ B1a cells (and parallel increase in CD5$^-$ IL-10–GFP$^+$ B1b cells) in 2-mo-old $lyn^{-/-}tiger$ compared with $tiger$ mice (percentage of CD5$^+$ IL-10–GFP$^+$ B1a cells in $tiger$ was 58% ± 3 vs. 39% ± 4 in $lyn^{-/-}tiger$ mice; $P < 0.03$; $n = 3$). The percentage of IL-10–GFP$^+$ B cells with a Fo or marginal zone (MZ) phenotype was significantly reduced in the spleens of $lyn^{-/-}tiger$ mice (Table 1), in agreement with the lower frequency of these B-cell types in $lyn^{-/-}$ mice (10).

The frequency and the number of splenic IL-10–GFP$^+$ T cells and myeloid cells was also elevated in $lyn^{-/-}tiger$ compared with control $tiger$ mice (Fig. 4B and Fig. S3 B, D, and E). Among T-cell subpopulations, CD4$^+$ T cells were the most representative IL-10–GFP$^+$ T cells in the spleens of control $tiger$ and $lyn^{-/-}tiger$ mice (Table 1 and Fig. S3D). Surprisingly, among the splenic IL-10–GFP$^+$ T cells, only approximately 10% were CD4$^+$CD25$^+$ Tregs in both control $tiger$ and $lyn^{-/-}tiger$ mice (Table 1 and Fig. S3D). Among the myeloid cell population tested, neutrophils and monocytes/macrophages were the most representative IL-10–GFP$^+$ CD11b$^+$ in both control $tiger$ and $lyn^{-/-}tiger$ mice (Table 1).

The fact that B cells represented the largest population of IL-10–GFP$^+$ splenic cells in $lyn^{-/-}tiger$ mice at an early stage of disease development was of particular interest to us. We first investigated whether this increased frequency, as well the different phenotype, of IL-10–GFP$^+$ B cells present in $lyn^{-/-}tiger$ mice was a result of intrinsic effects caused by the lack of Lyn in these cells or was caused by the overall inflammatory environment present in these animals. To address this question, we purified WT CD19$^+$ B cells (carrying the CD45.2 congenic marker) from control $tiger$ mice and adoptively transferred these

cells into 6-mo-old congenic B6 or $lyn^{-/-}$ animals carrying the CD45.1 allele. Interestingly, we found that the frequency of splenic IL-10–GFP$^+$ CD45.2$^+$ B cells, generated out of the total CD45.2$^+$ donor B cells, was significantly higher following transfer into congenic $lyn^{-/-}$ versus B6 mice (percentage of IL-10–GFP$^+$ CD45.2$^+$ B cells in B6 was 3% ± 0.3 vs. 12% ± 2.6 in $lyn^{-/-}$ mice; $P < 0.02$; $n = 4$; Fig. 4C). Unexpectedly, the transferred total donor CD45.2$^+$ cells (IL-10–GFP$^-$ and IL-10–GFP$^+$) assumed a phenotype that resembled the Lyn-deficient B-cell phenotype, manifesting a reduced frequency of Fo and MZ B cells and an increased frequency of plasma cells/plasmablasts (Fig. 4C). Consistently, the majority of donor WT IL-10–GFP$^+$ B cells recovered from the spleens of host $lyn^{-/-}$ mice were plasma cells/plasmablasts, T1,2 B cells, and B1a/b B cells, and they showed a phenotype similar to the splenic $lyn^{-/-}$ IL-10–GFP$^+$ B cells present in $lyn^{-/-}tiger$ mice (Fig. 4C and Table 1). Splenic donor WT IL-10–GFP$^+$ B cells developed in host B6 mice showed the same phenotype as splenic IL-10–GFP$^+$ B cells present in control $tiger$ mice (Fig. 4C and Table 1). These data suggest that the inflammatory environment present in $lyn^{-/-}$ mice dramatically affects the frequency and the phenotype of B cells, including the differentiation of IL-10–producing B cells.

Consistent with the increased frequency of IL-10–GFP$^+$ B cells observed in the spleens of $lyn^{-/-}tiger$ mice, we found that $lyn^{-/-}$ B cells released increased amounts of IL-10 compared with WT B cells after stimulation with LPS, CpG oligonucleotide, or anti-CD40 Abs (Fig. 4D), stimuli that have been previously described to induce IL-10 production by B cells (29, 30).

B Cells, but Not T or Myeloid Cells, Are the Crucial Source of IL-10 Able to Reduce Disease Development in Double-Mutant $lyn^{-/-}IL$-$10^{-/-}$ Mice. In view of the early expansion of IL-10–producing B cells in $lyn^{-/-}$ mice, we investigated whether adoptive transfer of WT or $lyn^{-/-}$ IL-10–sufficient B cells could reduce the inflammatory and autoimmune disease developed by $lyn^{-/-}IL$-$10^{-/-}$ mice. We first adoptively transferred 10×10^6 WT CD19$^+$ B cells, isolated from the spleen and lymph nodes of 2-mo-old sex-matched congenic WT animals, into 2-mo-old $lyn^{-/-}IL$-$10^{-/-}$ mice. Experimental animals were then killed and screened for disease

Table 1. Phenotype of IL-10-GFP$^+$ cells in $lyn^{-/-}$ mice

	2 mo		4 mo		6 mo	
Genotype	WT	$lyn^{-/-}$	WT	$lyn^{-/-}$	WT	$lyn^{-/-}$
Phenotype of IL-10–GFP$^+$ B cell, %						
Follicular (CD19$^+$CD23$^+$CD21^{int})	41 ± 3	6 ± 0.8*	47 ± 4	10 ± 1*	45 ± 6	7 ± 1.5*
MZ (CD19$^+$CD23$^-$CD21^{high})	8 ± 1.8	1 ± 0.4†	12 ± 2	1 ± 0.5*	10 ± 0.6	1 ± 0.2*
Transitional T1+T2 (CD19$^+$AA4/CD93$^+$)	12 ± 0.8	19 ± 2†	14 ± 2	23 ± 1†	7 ± 1.3	19 ± 1.4†
Plasma cells/plasmablasts (CD19/B220$^{low/-}$CD138$^+$)	19 ± 5	49 ± 4*	18 ± 4	55 ± 2*	25 ± 3	56 ± 3*
B1 a/b (CD19$^+$ CD138$^-$CD21$^-$CD23$^-$CD43$^+$CD5$^{+/-}$)	11 ± 2	23 ± 4†	9 ± 1	17 ± 2†	7 ± 0.8	16 ± 1†
Phenotype of IL-10–GFP$^+$ T cells, %						
CD4$^+$ (TCRβ$^+$CD4$^+$)	83 ± 2	70 ± 6	85 ± 4	59 ± 5†	73 ± 2.2	58 ± 5†
Treg (TCRβ$^+$CD4$^+$CD25$^+$FoxP3$^+$)	14 ± 1.4	12 ± 1.6	11 ± 1	9 ± 1.1	9 ± 2	8 ± 2.3
CD8$^+$(TCRβ$^+$CD8$^+$)	17 ± 1	29 ± 4	15 ± 1.5	38 ± 5†	27 ± 2.3	39 ± 6†
Phenotype of IL-10–GFP$^+$ myeloid cells, %						
Neutrophils (CD11b$^+$Ly6G$^+$)	24 ± 4	24 ± 3.2	23 ± 2	20 ± 1	23 ± 6	26 ± 1
Monocytes/macrophages (CD11b$^+$F4/80$^+$)	26 ± 8	30 ± 4	33 ± 2	35 ± 2	35 ± 8	32 ± 4
mDC (CD11b$^+$CD11c^{high})	8 ± 0.9	15 ± 2.7†	9 ± 1	14 ± 2†	8.5 ± 1	13 ± 1.6†

Single-cell suspensions of spleens from 2-mo-old control $tiger$ or $lyn^{-/-}tiger$ mice were prepared and stained for flow cytometric analysis as described in Methods. The gates designed to analyze GFP expression were set by using regular WT or $lyn^{-/-}$ mice as GFP$^-$ controls. The phenotype of IL-10-GFP$^+$ B cells (out of total CD19$^+$ plus CD19/B220$^{low/-}$CD138$^+$IL-10-GFP$^+$ B cells), IL-10-GFP$^+$ T cells (out of total TCRβ$^+$IL-10-GFP$^+$ T cells) and IL-10-GFP$^+$ myeloid cells (out of total CD19$^-$TCRβ$^-$CD11b$^+$IL-10-GFP$^+$ myeloid cells) was detected by analysis of the expression of the indicated markers. Data are representative of 5–6 mice for each genotype and are expressed as mean ± SEM. mDC, myeloid DC.
*$P < 0.01$, $^†P < 0.05$.

development 2 to 3 mo after the transfer. At this time point, 5% to 10% of the total B-cell population present in the spleen and lymph nodes of the host $lyn^{-/-}IL\text{-}10^{-/-}$ mice were transferred WT donor B cells. The development of splenomegaly, myeloproliferation, T-cell expansion, and T-cell activation was significantly reduced in $lyn^{-/-}IL\text{-}10^{-/-}$ mice that received WT B cells compared with untreated control $lyn^{-/-}IL\text{-}10^{-/-}$ mice (Fig. 5 A–C). Adaptive transfer of WT B cells was also able to significantly reverse the down-regulation of Foxp3 expression in $IL\text{-}10^{-/-}$ Tregs present in $lyn^{-/-}IL\text{-}10^{-/-}$ mice (Fig. 5D). Adoptive transfer of WT B cells did not alter the autoantibody titers in the $lyn^{-/-}IL\text{-}10^{-/-}$ mice. In contrast, $lyn^{-/-}IL\text{-}10^{-/-}$ mice that received adoptive transfers of $IL\text{-}10^{-/-}$ B cells developed similar levels of disease compared with untreated $lyn^{-/-}IL\text{-}10^{-/-}$ mice, indicating that the protective effect obtained with adoptive transfers of WT B cells was IL-10–dependent (Fig. 5).

We next performed adoptive transfers of 5×10^6 CD19$^+$ $lyn^{-/-}$ B cells into $lyn^{-/-}IL\text{-}10^{-/-}$ mice. Despite technical difficulties with this experiment as a result of the reduced number of B cells present in the donor $lyn^{-/-}$ mice, $lyn^{-/-}$ B cells were also able to significantly reduce disease development in $lyn^{-/-}IL\text{-}10^{-/-}$ recipients (Fig. S4 A–C).

CD4$^+$ Tregs represent another major source of IL-10 (21), and might also modulate the inflammatory/autoimmune disease in this model. Thus, we performed adoptive transfers of these cells into $lyn^{-/-}IL\text{-}10^{-/-}$ mice. WT CD4$^+$ Tregs were isolated from CD8$^+$ T-cell–deficient congenic mice, expanded in vitro (28, 40), then transferred into $lyn^{-/-}IL\text{-}10^{-/-}$ mice (10×10^6 cells per mouse). WT CD4$^+$ Tregs were unable to suppress disease development in the $lyn^{-/-}IL\text{-}10^{-/-}$ mice, despite the fact that 5% to 8% of the CD4$^+$ Tregs were expressing the congenic marker of the transferred donor WT Tregs in the recipients (Fig. S4 D–F). A similar down-regulation of Foxp3 expression was observed in the donor WT Tregs and the host $IL\text{-}10^{-/-}$ Tregs present in $lyn^{-/-}IL\text{-}10^{-/-}$ mice. Moreover, adoptive transfers of total TCRβ$^+$ WT or $IL\text{-}10^{-/-}$ T cells isolated from the spleen and lymph nodes of WT or $IL\text{-}10^{-/-}$ mice, respectively, did not reduce disease development in $lyn^{-/-}IL\text{-}10^{-/-}$ mice (Fig. S4 G–I), further excluding a possible role of other T-cell subsets as an important source of IL-10 in $lyn^{-/-}$ mice.

Finally, we investigated whether myeloid cells are an important source of IL-10 in our model. For this purpose, we generated chimeric mice by reconstituting, as previously described (14), the hematopoietic system of lethally irradiated WT or $IL\text{-}10^{-/-}$ animals with bone marrow from $lyn^{-/-}rag^{-/-}$ mice mixed, in a ratio of 75% to 25%, with WT or $IL\text{-}10^{-/-}$ bone marrow. With this experimental approach, we obtained $lyn^{-/-}rag^{-/-}$+WT chimeras (in which the majority of myeloid cells were Lyn-deficient and every cell type, including myeloid cells, were IL-10–sufficient) or $lyn^{-/-}rag^{-/-}$+$IL\text{-}10^{-/-}$ chimeras (in which the majority of myeloid cells were Lyn-deficient and IL-10–sufficient, whereas all other cell types were IL-10–deficient). As previously demonstrated, the $lyn^{-/-}rag^{-/-}$+WT chimeras developed, at approximately 6 to 8 mo of age, a lupus-like disease that strongly resembled the disease developed by regular $lyn^{-/-}$ mice (14); however, the $lyn^{-/-}rag^{-/-}$+$IL\text{-}10^{-/-}$ chimeras developed much more severe and accelerated disease than the $lyn^{-/-}rag^{-/-}$+WT control chimeras (Fig. S4 J–L). These results indicate that IL-10 secretion by $lyn^{-/-}$ myeloid cells alone was not sufficient to reduce disease exacerbation caused by the lack of IL-10 in the lymphoid and stromal compartments in the Lyn-deficient model of autoimmunity.

Discussion

The role of IL-10 in the pathogenesis of SLE remains controversial (20, 41). In the present study, we use $lyn^{-/-}$ mice as a model of SLE and demonstrate that IL-10 plays a crucial role down-regulating the inflammatory component of the disease caused by myeloid and T-cell activation, while minimally affecting autoantibody production by B cells. Because of increased myeloid and T-cell activation/proliferation, $lyn^{-/-}IL\text{-}10^{-/-}$ double-mutant mice developed dramatic splenomegaly and lymphadenopathy, increased proinflammatory cytokine production, and tissue inflammation leading to severe end-organ damage and early mortality. We found that B cells were the main IL-10–producing cells in the spleen of $lyn^{-/-}$ mice especially at the initial stage of disease development. Interestingly, the expansion and the phenotype of IL-10–producing B cells in $lyn^{-/-}$ mice seemed to be a compensatory response to the inflammatory environment rather than an intrinsic effect of the lack of Lyn kinase in these cells. This conclusion is based on the observation that WT B cells adoptively transferred into $lyn^{-/-}$ hosts manifested an increased differentiation into IL-10–producing B cells that assumed a similar phenotype to endogenous $lyn^{-/-}$ IL-10–producing B cells. Adoptive transfer of IL-10–sufficient, but not IL-10–deficient, WT or $lyn^{-/-}$ B cells was able to reduce the disease development in $lyn^{-/-}IL\text{-}10^{-/-}$ mice. IL-10 secretion by B cells was also crucial to sustain Foxp3 expression in Tregs during disease development. In contrast, IL-10 production by T cells (including purified Tregs) or myeloid cells was not sufficient to reduce disease development in this model. Together these data suggest a dominant role of IL-10–producing B cells over Tregs (or other IL-10–producing cells) as critical source of IL-10 required to limit disease progression in the Lyn-deficient model of autoimmunity.

There are several possible mechanisms for the immunosuppressive effect of IL-10 on disease development in $lyn^{-/-}$ mice. IL-10 is crucial for inhibition of IFN-γ– and IL-17–producing T cells, which are known to promote inflammation and autoimmune diseases (42). Furthermore, IL-10 deficiency also results in a dramatically increased production of proinflammatory mediators, such as IL-6 and IL-1, which can induce down-regulation of Foxp3 expression in CD4$^+$ Tregs (23, 43, 44). The latter phenomenon can lead to the loss of Treg function (25), so it is likely that an important immunosuppressive role of IL-10 is to maintain the ability of the expanded CD4$^+$ Tregs to restrain disease development in $lyn^{-/-}$ mice (37). IL-10 also clearly limits the expansion of hyperactivated myeloid cells producing elevated amounts of proinflammatory cytokines that promote the establishment of pathogenic cross-talk between myeloid cells and T cells (14). Our data are consistent with a protective role of IL-10 observed in other mouse models of SLE-like disease, including IL-10–deficient MLR-Fas^{lpr} mice (45) and IL-10–overexpressing B6.Sle1.Sle2.Sle3 mice (46), but disagree with the pathogenic role of IL-10 demonstrated after administration of neutralizing anti–IL-10 antibody in New Zealand Black/White F1 hybrid mice (47). Several hypotheses attempted to explain these discrepancies, including the possibility that the positive and negative regulatory effects of IL-10 might differ depending on the timing of IL-10 overproduction, the levels of expression, or the cell source of IL-10 (45, 46). Our data suggest that mouse models with a strong T-cell pathogenic component are more likely to develop worse disease following IL-10 reduction.

A surprising finding of this study is the dominance of B cells over T cells (in particular Tregs) and myeloid cells as a crucial source of IL-10 able to suppress disease in $lyn^{-/-}IL\text{-}10^{-/-}$ mice. There could be several explanations for this, including better migration of IL-10–producing B cells to inflammatory niches (e.g., in the myeloid cell-rich bone marrow), more effective "presentation" of IL-10 by B cells, or a better ability of the latter cells, compared with other cell subsets, to produce this cytokine in response to the inflammatory environment present in $lyn^{-/-}$ mice. It is also possible that B-cell–derived IL-10 is needed for subsequent development of other IL-10–producing cells, including Tregs. B-cell–derived IL-10 may be especially important in maintaining Foxp3 expression in Tregs, which explains why Treg transfers into the $lyn^{-/-}IL\text{-}10^{-/-}$ model failed to restrain disease but such transfers are effective in limiting SLE-like disease in
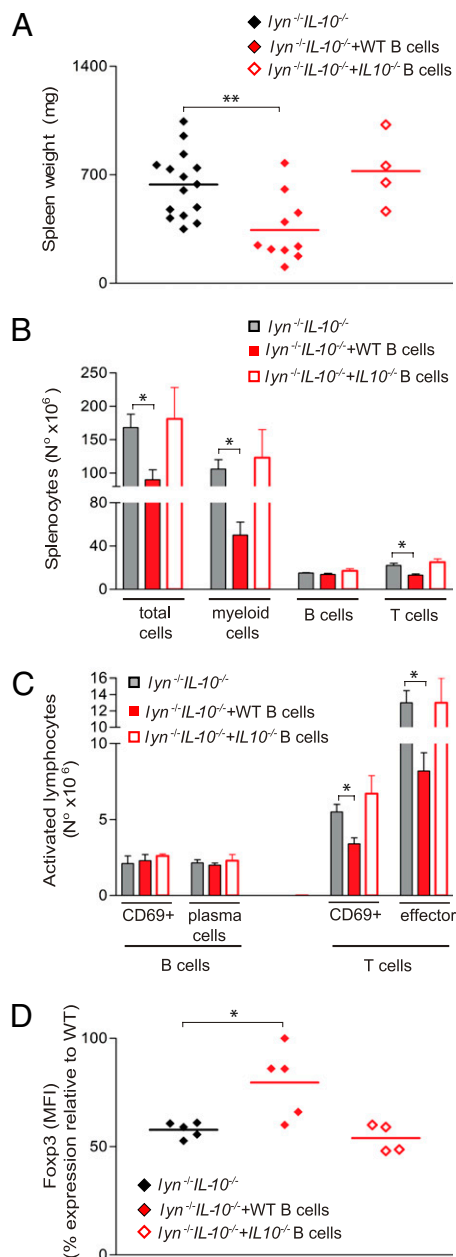
Fig. 5. B-cell–derived IL-10 is sufficient to reduce disease development in $lyn^{-/-}$ IL-$10^{-/-}$ mice. Two-month-old $lyn^{-/-}IL$-$10^{-/-}$ mice were injected with WT or IL-$10^{-/-}$ B cells (10×10^6 CD19$^+$ B cells per mouse) isolated from spleen and lymph nodes of 2-mo-old WT or IL-$10^{-/-}$ animals. Two to 3 mo after the adoptive transfer, mice were killed and analyzed for signs of disease development. (*A*) Each symbol represents the weight of an individual spleen from $lyn^{-/-}IL$-$10^{-/-}$ mice untreated or treated by adoptive transfer of WT or IL-$10^{-/-}$ B cells. (*B–D*) Single-cell suspensions of spleens were prepared, counted, and stained for flow cytometric analysis. (*B*) The absolute number of total myeloid (CD11b$^+$), total B (CD19$^+$ plus CD19/B220$^{low/-}$CD138$^+$ cells), and T (TCRβ$^+$) cells is reported. (*C*) The absolute number of CD19$^+$CD69$^+$ and CD19/B220$^{low/-}$CD138$^+$ (plasma cells/plasmablasts), TCRβ$^+$CD69$^+$, and TCRβ$^+$CD44^{high}CD62L$^-$ (effector cells) is reported as evidence of B- and T-cell activation. Data from WT B-cell transfers are pooled from three independent end-point experiments, whereas data from IL-$10^{-/-}$ B-cell transfers were pooled from two end-point experiment. Data are expressed as mean ± SEM (n = 4–15 mice per group). (*D*) Each symbol represents the MFI of Foxp3 expression in splenic CD4$^+$CD25$^+$Foxp3$^+$ Tregs (calculated as percentage of MFI expression relative to WT levels for each experiment) from individual $lyn^{-/-}$ IL-$10^{-/-}$ mice untreated or treated by adoptive transfers of WT or IL-$10^{-/-}$ B cells. Data are pooled from three independent end-point experiments. Statistical differences of untreated $lyn^{-/-}IL$-$10^{-/-}$ mice vs. $lyn^{-/-}IL$-$10^{-/-}$ mice treated with adoptive transfers of WT or IL-$10^{-/-}$ B cells are reported (*P < 0.05).

other autoimmune models, such as New Zealand Black/White F1 hybrid mice, in which IL-10 is present (28). This function of IL-10–producing B cells on Tregs could be direct or indirect through the inhibition of proinflammatory cytokine production by other T cells or myeloid cells.

Our data are consistent with the emerging picture of a negative regulatory role of Breg subsets in the modulation of autoimmunity, including, more recently, SLE (29–31, 33–35, 48). Nevertheless, besides the general agreement on the ability of Bregs to produce IL-10, the categorization of these cells into specific subsets is complicated by the heterogeneous cell markers identified so far by different research groups (29–31, 48). Among the best characterized Breg subsets (found to date mainly in mouse spleen), CD1d^{high}CD5$^+$ Bregs (also known as B10 cells) have been identified by IL-10 intracellular staining following stimulation ex vivo with phorbol myristate acetate (PMA)/ionomycin/LPS in the presence of brefeldin A (49), and CD1d^{high}CD23$^+$IgM^{high}CD21^{high} "transitional" type 2 (T2)-MZ Bregs have been mainly identified by IL-10 intracellular staining following stimulation ex vivo with anti-CD40 followed by PMA/ionomycin/brefeldin A stimulation (50). Other IL-10–producing B-cell subsets have also been described, such as CD1d^{high}C-D23$^-$IgM^{high}CD21^{high} MZ B cells and CD5$^+$ B1a cells (29–31). In control t$iger$ and $lyn^{-/-}tiger$ mice, we found that splenic IL-10–producing B cells were distributed within several different subsets, including follicular, plasma cells/plasmablasts, B1a/b, and transitional T1 and T2 B cells, although the frequency of the different subsets was different in WT vs. $lyn^{-/-}$ mice. As we did not identify a specific "Breg" subset, we decided to refer these cells "IL-10–producing B cells" rather than Bregs, as this latter term defines these cells as a distinct lineage. Our data were consistent with the variety of splenic IL-10–producing B-cell subsets observed with another IL-10–GFP reporter system (39). We were surprised, however, to observe that WT B cells transferred into $lyn^{-/-}$ recipient mice differentiated into B cells resembling endogenous subsets and showed an expansion of IL-10–producing B cells compared with WT hosts. These data suggest that the host environment has a significant effect on B-cell maturation/activation, including skewing the differentiation of IL-10–producing B cells resulting in different cell surface marker expression. Even though it is not clear which are the specific inflammatory mechanisms or cytokines that are driving the differentiations of B cells in different IL-10–producing cell subsets, we tend to exclude an important role of IL-10 itself in this function as the deficiency of this cytokine did not significantly affect the overall B-cell phenotype in $lyn^{-/-}IL$-$10^{-/-}$ double-mutant mice compared with $lyn^{-/-}$ single-mutant mice. Therefore, the ability to produce IL-10 is likely a general property of activated B cells that may not be restricted to a defined lineage. Indeed, the dramatic expansion of IL-10–producing B cells in $lyn^{-/-}$ mice (even in the face of overall lower B-cell numbers, with a skewed distribution of immature cells and plasmablasts) may be a compensatory response to attempt to limit the myeloid/T-cell–driven inflammation. However, as the relative expansion of IL-10–producing B cells in $lyn^{-/-}$ mice begins at 2 mo of age, before the onset of obvious disease [which occurs at 4–6 mo (14)], it is also possible that the deregulated signaling pathways intrinsic to $lyn^{-/-}$ B cells may favor IL-10–producing B-cell development (to the same extent they contribute to the overall $lyn^{-/-}$ B-cell phenotype). Dissecting the molecular details of how the intracellular signaling disruption in $lyn^{-/-}$ B cells may favor IL-10–producing B-cell development remains a goal of future work.

In conclusion, our data suggest that IL-10, and in particular IL-10–producing B cells, plays an important role in suppressing inflammation and establishing anti-inflammatory networks that are crucial to maintain the balance between pathogenic T-cell subsets and beneficial Treg cells in inflammation associated with SLE-like

disease (51, 52). Caution should be used when interpreting the elevated levels of IL-10 (including elevated production of IL-10 by B cells) observed in patients with SLE (19, 20), as these may be a reflection of disease activity, i.e., a compensatory function of B cells during an inflammatory state, rather than an underlying cause of systemic autoimmunity. Despite the paucity of data on the existence of IL-10–producing B-cell subsets in humans, the existence of IL-10–producing B-cell subsets in healthy donors and in patients with autoimmune disease, including SLE, has been recently described (53, 54). Furthermore, altered Treg functions, including Foxp3 down-regulation, have also been described in patients with SLE (27, 55). In view of the fact that Treg cellular therapies are entering clinical trials, our data suggest that, in autoimmune diseases with a strong inflammatory component and high levels of proinflammatory cytokines, the transfer of IL-10–producing B cells might need to be considered as an additional/alternative therapeutic approach.

Methods

Mice. $Lyn^{-/-}$ and $lyn^{-/-}rag^{-/-}$ mice were previously established and backcrossed onto the C57BL/6 (B6, carrying the CD45.2 allele) background for 15 generations (14, 56). $Lyn^{-/-}$ mice on the B6 background but carrying the CD45.1 allele were generated by cross-breeding with congenic WT mice carrying the CD45.1 allele on the B6 background (Taconic Farms). Age-matched WT B6 mice and $IL-10^{-/-}$ (carrying the CD45.2 allele) were purchased from Charles River Laboratories and Jackson Laboratory, respectively. $Lyn^{-/-}IL-10^{-/-}$ double-mutant mice were generated by cross-breeding $lyn^{-/-}$ mice with $IL-10^{-/-}$ mice. $Lyn^{-/-}tiger$ mice were generated by cross-breeding $lyn^{-/-}$ mice with IL-10 reporter GFP knock-in tiger mice [gift from R. A. Flavell, Yale University, New Haven, CT (38)]. Bone marrow-derived chimeras were generated as previously described (14). To generate sufficient numbers of recipient animals to perform the adoptive transfer studies, we generated $lyn^{-/-}IL-10^{-/-}$ bone marrow chimeric mice ($lyn^{-/-}IL-10^{-/-}$ chimeras) by reconstituting the hematopoietic system of $IL-10^{-/-}$ mice with bone marrow isolated from $lyn^{-/-}IL-10^{-/-}$ animals. Lethally irradiated B6 mice reconstituted with 100% WT or $lyn^{-/-}$ cells and lethally irradiated $IL-10^{-/-}$ mice reconstituted with 100% $IL-10^{-/-}$ cells were also generated as controls. The overall inflammatory/autoimmune disease developed by $lyn^{-/-}IL-10^{-/-}$ chimeric mice was comparable to the disease developed by regular $lyn^{-/-}IL-10^{-/-}$ mice, although we did observed some variability in the severity of the disease between different experimental sets of chimeras. However, despite this variability, the dramatic exacerbation of disease development in the $lyn^{-/-}IL-10^{-/-}$ chimeric mice was always evident compared with $lyn^{-/-}$ and $IL-10^{-/-}$ single chimeric mice. Finally, $lyn^{-/-}rag^{-/-}$+WT chimeras (in which the majority of the myeloid cells were Lyn-deficient and every cell type, including myeloid cells, were IL-10–sufficient) were generated by reconstituting lethally irradiated B6 mice with a "pool" of bone marrow cells containing 75% cells from $lyn^{-/-}rag^{-/-}$ mice mixed with 25% cells from WT mice, whereas $lyn^{-/-}rag^{-/-}$+$IL-10^{-/-}$ chimeras (in which the majority of myeloid cells were Lyn-deficient and IL-10–sufficient, whereas every other cell type was IL-10–deficient) were generated by reconstituting $IL-10^{-/-}$ mice with a pool of bone marrow cells containing 75% cells from $lyn^{-/-}rag^{-/-}$ mice mixed with 25% cells from $IL-10^{-/-}$ mice. All host and donor mice used to generate the bone marrow chimeras were 8 to 12 wk old. All animals were kept in a specific pathogen-free facility at University of California, San Francisco, and used according to protocols approved by the University of California, San Francisco, committee on animal research.

Flow Cytometry (FACS). Single-cell suspensions from spleens and/or lymph nodes were prepared and stained as previously described (14) with the following additional anti-mouse FITC-conjugated, allophycocyanin-conjugated, phycoerythrin-conjugated, or allophycocyanin-Cy7–conjugated Abs: CD25 (PC61.5) CD4 (GK1.5) CD8 (53-6.7) CD5 (53-7.3) CD43 (S7), CD93 (AA4.1), Ly6G (1A8), CD5 (53-7.3), all from eBiosciences or BD Pharmingen. Foxp3 detection in CD4$^+$CD25$^+$ Tregs was performed by intracellular staining by using the Foxp3 Fixation/Permeabilization kit according to the manufacturer's instruction and anti-Foxp3 Abs (FJK-16.s; eBiosciences). For intracellular anal-

ysis of cytokine production by flow cytometry, splenocytes were stimulated as follows: 4 h with PMA (50 ng/mL) and ionomycin (1 μg/mL; Sigma-Aldrich) in the presence of 3 μg/mL brefeldin A (eBiosciences) for IFN-γ and IL-17 production by TCRβ$^+$ T cells; and 6 h with 5 μg/mL LPS in the presence of 3 μg/mL brefeldin A (eBiosciences) for IL-6, TNF-α, IL-10, and IL-12/IL-23 p40 production by CD11b$^+$ myeloid cells. The following Abs were used for the intracellular cytokine staining: IFN-γ (XMG1.2), IL-17 (17B7), IL-10 (JES5), IL-6 (MP5-20F3), TNF-α (MP6XT22), and IL-12/IL-23 p40 (C17.8; all from eBiosciences).

Cell Isolation and Culture. Total mouse splenocytes or splenic DCs and macrophages were isolated and cultured as previously described (14). B cells were isolated by sorting with a MoFlo High-Speed Sorter (purity of >98%; Dako), suspended in RPM1-1640 complete medium, plated as described earlier, and incubated at 37 °C in 5% CO$_2$ in the presence or absences of 5 μg/mL LPS, CpG oligodeoxynucleotide 1826 containing a phosphorothioate backbone (CpG; Integrated DNA Technologies), or anti-CD40 Abs (3/23; BD Pharmingen) for 24 h. Cells were then collected and centrifuged at 350 × g for 5 min, and the resulting supernatants stored at a temperature of −20 °C or lower.

Tissue Histological Analysis and Kidney Immunofluorescence Staining. H&E or immunofluorescence staining of kidney, liver, lung, and colon tissues were performed as previously described (14).

Cytokine Assays. BAFF concentrations in sera were measured by ELISA as described before (14). All other indicated cytokine concentrations were detected in sera by using Cytokine Multiplex Kits for the Luminex technology according to the manufacturer's protocol (Millipore). IL-10 in cell-free supernatants was also measured by ELISA by using cytokine-specific paired Abs (BD Pharmingen) according to the manufacturer's protocol.

RNA Extractions and TaqMan Real-Time PCR Analysis. RNA extractions from purified cells or total spleen, retrotranscription and quantitative real time-PCR were performed as previously described (14). BAFF and HPRT primer pairs and probes were described previously (14). IL-10 and IL-6 primers pairs and probes used were from Applied Biosystems. Values of BAFF, IL-6, or IL-10 mRNA were normalized to the values of HPRT mRNA in each sample.

Serum Ig and Autoantibody Measurement. Levels of total serum Ig, anti-dsDNA, and anti-RNA Ig ELISA were performed as previously described (14).

Adoptive Cell Transfers. CD19$^+$TCRβ$^-$ B cells and TCRβ$^+$CD19$^-$ T cells were purified by sorting from single-cell suspensions of spleens and lymph nodes of 2-mo-old congenic WT (CD45.1) or $IL-10^{-/-}$ (CD45.2) mice as described in *Cell Isolation and Culture*. Purified WT or $IL-10^{-/-}$ B or T cells (10 × 10^6) were suspended in a total of 200 μL of saline solution and injected i.v. into $lyn^{-/-}IL-10^{-/-}$ mice (CD45.2). Thanks to the expression of the CD45.1 congenic marker, we could analyze at the time the animals were killed the number/frequency of the surviving WT B and T donor cells transferred into $lyn^{-/-}IL-10^{-/-}$ host mice. As we have not crossed the $IL-10^{-/-}$ mouse onto the CD45.1 genetic background, we could not perform a similar follow-up for the transferred donor $IL-10^{-/-}$ B and T cells. However, it is unlikely that these cells have an intrinsic survival defect, as they expand and function normally in $IL-10^{-/-}$ mice. Adoptive B-cell transfers of 5 × 10^6 CD19$^+$TCRβ$^-$ B cells isolated from spleens and lymph nodes of 2-mo-old $lyn^{-/-}$ (CD45.1) or $lyn^{-/-}IL-10^{-/-}$ (CD45.2) mice were also performed. For adoptive Treg transfers, sorted CD4$^+$CD25$^+$CD62L^{high} Tregs, purified from CD8$^+$ T-cell–deficient congenic mice (CD45.1), were cultured by using the protocol described previously (28). After 10 d of culture, expanded Tregs were assessed for Foxp3, washed, suspended in saline solution, and injected i.v (10 × 10^6/200 μL) into $lyn^{-/-}IL-10^{-/-}$ animals. Two to 3 mo after adoptive transfers, animals were killed and analyzed for disease development.

Statistical Analysis. Statistical significance was determined with the unpaired two-tailed Student t test.

1. Crispín JC, et al. (2010) Pathogenesis of human systemic lupus erythematosus: Recent advances. *Trends Mol Med* 16:47–57.
2. Jacob N, Stohl W (2010) Autoantibody-dependent and autoantibody-independent roles for B cells in systemic lupus erythematosus: Past, present, and future. *Autoimmunity* 43:84–97.
3. Crispín JC, Kyttaris VC, Terhorst C, Tsokos GC (2010) T cells as therapeutic targets in SLE. *Nat Rev Rheumatol* 6:317–325.
4. Katsiari CG, Liossis SN, Sfikakis PP (2010) The pathophysiologic role of monocytes and macrophages in systemic lupus erythematosus: A reappraisal. *Semin Arthritis Rheum* 39:491–503.

5. Seitz HM, Matsushima GK (2010) Dendritic cells in systemic lupus erythematosus. *Int Rev Immunol* 29:184–209.
6. Rönnblom L, Elkon KB (2010) Cytokines as therapeutic targets in SLE. *Nat Rev Rheumatol* 6:339–347.
7. Richez C, Blanco P, Rifkin I, Moreau JF, Schaeverbeke T (2011) Role for toll-like receptors in autoimmune disease: The example of systemic lupus erythematosus. *Joint Bone Spine* 78:124–130.
8. Marshak-Rothstein A (2006) Toll-like receptors in systemic autoimmune disease. *Nat Rev Immunol* 6:823–835.
9. Morel L (2010) Genetics of SLE: Evidence from mouse models. *Nat Rev Rheumatol* 6:348–357.
10. Xu Y, Harder KW, Huntington ND, Hibbs ML, Tarlinton DM (2005) Lyn tyrosine kinase: Accentuating the positive and the negative. *Immunity* 22:9–18.
11. Scapini P, Pereira S, Zhang H, Lowell CA (2009) Multiple roles of Lyn kinase in myeloid cell signaling and function. *Immunol Rev* 228:23–40.
12. Lu R, et al.; BIOLUPUS and GENLES Multicenter Collaborations (2009) Genetic associations of LYN with systemic lupus erythematosus. *Genes Immun* 10:397–403.
13. Chan VW, Meng F, Soriano P, DeFranco AL, Lowell CA (1997) Characterization of the B lymphocyte populations in Lyn-deficient mice and the role of Lyn in signal initiation and down-regulation. *Immunity* 7:69–81.
14. Scapini P, et al. (2010) Myeloid cells, BAFF, and IFN-gamma establish an inflammatory loop that exacerbates autoimmunity in Lyn-deficient mice. *J Exp Med* 207:1757–1773.
15. Charles N, Hardwick D, Daugas E, Illei GG, Rivera J (2010) Basophils and the T helper 2 environment can promote the development of lupus nephritis. *Nat Med* 16:701–707.
16. Sabat R, et al. (2010) Biology of interleukin-10. *Cytokine Growth Factor Rev* 21:331–344.
17. Mosser DM, Zhang X (2008) Interleukin-10: New perspectives on an old cytokine. *Immunol Rev* 226:205–218.
18. Saraiva M, O'Garra A (2010) The regulation of IL-10 production by immune cells. *Nat Rev Immunol* 10:170–181.
19. Beebe AM, Cua DJ, de Waal Malefyt R (2002) The role of interleukin-10 in autoimmune disease: systemic lupus erythematosus (SLE) and multiple sclerosis (MS). *Cytokine Growth Factor Rev* 13:403–412.
20. Llorente L, Richaud-Patin Y (2003) The role of interleukin-10 in systemic lupus erythematosus. *J Autoimmun* 20:287–289.
21. Maynard CL, Weaver CT (2008) Diversity in the contribution of interleukin-10 to T-cell-mediated immune regulation. *Immunol Rev* 226:219–233.
22. Campbell DJ, Koch MA (2011) Phenotypical and functional specialization of FOXP3+ regulatory T cells. *Nat Rev Immunol* 11:119–130.
23. Murai M, et al. (2009) Interleukin 10 acts on regulatory T cells to maintain expression of the transcription factor Foxp3 and suppressive function in mice with colitis. *Nat Immunol* 10:1178–1184.
24. Zhou X, Bailey-Bucktrout S, Jeker LT, Bluestone JA (2009) Plasticity of CD4(+) FoxP3(+) T cells. *Curr Opin Immunol* 21:281–285.
25. Wan YY, Flavell RA (2007) Regulatory T-cell functions are subverted and converted owing to attenuated Foxp3 expression. *Nature* 445:766–770.
26. Zhou X, et al. (2009) Instability of the transcription factor Foxp3 leads to the generation of pathogenic memory T cells in vivo. *Nat Immunol* 10:1000–1007.
27. Horwitz DA (2008) Regulatory T cells in systemic lupus erythematosus: past, present and future. *Arthritis Res Ther* 10:227.
28. Scalapino KJ, Tang Q, Bluestone JA, Bonyhadi ML, Daikh DI (2006) Suppression of disease in New Zealand Black/New Zealand White lupus-prone mice by adoptive transfer of ex vivo expanded regulatory T cells. *J Immunol* 177:1451–1459.
29. DiLillo DJ, Matsushita T, Tedder TF (2010) B10 cells and regulatory B cells balance immune responses during inflammation, autoimmunity, and cancer. *Ann N Y Acad Sci* 1183:38–57.
30. Lampropoulou V, et al. (2010) Suppressive functions of activated B cells in autoimmune diseases reveal the dual roles of Toll-like receptors in immunity. *Immunol Rev* 233:146–161.

31. Mauri C, Blair PA (2010) Regulatory B cells in autoimmunity: Developments and controversies. *Nat Rev Rheumatol* 6:636–643.
32. Neves P, et al. (2010) Signaling via the MyD88 adaptor protein in B cells suppresses protective immunity during Salmonella typhimurium infection. *Immunity* 33:777–790.
33. Blair PA, et al. (2009) Selective targeting of B cells with agonistic anti-CD40 is an efficacious strategy for the generation of induced regulatory T2-like B cells and for the suppression of lupus in MRL/lpr mice. *J Immunol* 182:3492–3502.
34. Haas KM, et al. (2010) Protective and pathogenic roles for B cells during systemic autoimmunity in NZB/W F1 mice. *J Immunol* 184:4789–4800.
35. Watanabe R, et al. (2010) Regulatory B cells (B10 cells) have a suppressive role in murine lupus: CD19 and B10 cell deficiency exacerbates systemic autoimmunity. *J Immunol* 184:4801–4809.
36. Tsantikos E, et al. (2010) Autoimmune disease in Lyn-deficient mice is dependent on an inflammatory environment established by IL-6. *J Immunol* 184:1348–1360.
37. Tsantikos E, et al. (2009) Perturbation of the CD4 T cell compartment and expansion of regulatory T cells in autoimmune-prone Lyn-deficient mice. *J Immunol* 183:2484–2494.
38. Kamanaka M, et al. (2006) Expression of interleukin-10 in intestinal lymphocytes detected by an interleukin-10 reporter knockin tiger mouse. *Immunity* 25:941–952.
39. Madan R, et al. (2009) Nonredundant roles for B cell-derived IL-10 in immune counter-regulation. *J Immunol* 183:2312–2320.
40. Tang Q, et al. (2004) In vitro-expanded antigen-specific regulatory T cells suppress autoimmune diabetes. *J Exp Med* 199:1455–1465.
41. Yap DY, Lai KN (2010) Cytokines and their roles in the pathogenesis of systemic lupus erythematosus: From basics to recent advances. *J Biomed Biotechnol* 2010:365083.
42. Damsker JM, Hansen AM, Caspi RR (2010) Th1 and Th17 cells: Adversaries and collaborators. *Ann N Y Acad Sci* 1183:211–221.
43. Pasare C, Medzhitov R (2003) Toll pathway-dependent blockade of CD4+CD25+ T cell-mediated suppression by dendritic cells. *Science* 299:1033–1036.
44. Yang XO, et al. (2008) Molecular antagonism and plasticity of regulatory and inflammatory T cell programs. *Immunity* 29:44–56.
45. Yin Z, et al. (2002) IL-10 regulates murine lupus. *J Immunol* 169:2148–2155.
46. Blenman KR, et al. (2006) IL-10 regulation of lupus in the NZM2410 murine model. *Lab Invest* 86:1136–1148.
47. Ishida H, et al. (1994) Continuous administration of anti-interleukin 10 antibodies delays onset of autoimmunity in NZB/W F1 mice. *J Exp Med* 179:305–310.
48. Lemoine S, Morva A, Youinou P, Jamin C (2009) Regulatory B cells in autoimmune diseases: How do they work? *Ann N Y Acad Sci* 1173:260–267.
49. Yanaba K, Bouaziz JD, Matsushita T, Tsubata T, Tedder TF (2009) The development and function of regulatory B cells expressing IL-10 (B10 cells) requires antigen receptor diversity and TLR signals. *J Immunol* 182:7459–7472.
50. Evans JG, et al. (2007) Novel suppressive function of transitional 2 B cells in experimental arthritis. *J Immunol* 178:7868–7878.
51. Leung S, et al. (2010) The cytokine milieu in the interplay of pathogenic Th1/Th17 cells and regulatory T cells in autoimmune disease. *Cell Mol Immunol* 7:182–189.
52. Littman DR, Rudensky AY (2010) Th17 and regulatory T cells in mediating and restraining inflammation. *Cell* 140:845–858.
53. Blair PA, et al. (2010) CD19(+)CD24(hi)CD38(hi) B cells exhibit regulatory capacity in healthy individuals but are functionally impaired in systemic Lupus Erythematosus patients. *Immunity* 32:129–140.
54. Iwata Y, et al. (2010) Characterization of a rare IL-10-competent B-cell subset in man that parallels mouse regulatory B10 cells. *Blood* 117:530–541.
55. Zhang B, Zhang X, Tang F, Zhu L, Liu Y (2008) Reduction of forkhead box P3 levels in CD4+CD25high T cells in patients with new-onset systemic lupus erythematosus. *Clin Exp Immunol* 153:182–187.
56. Pereira S, Lowell C (2003) The Lyn tyrosine kinase negatively regulates neutrophil integrin signaling. *J Immunol* 171:1319–1327.